

Rejuvenation and Memory in model Spin Glasses in 3 and 4 dimensions.

S. Jiménez,^{1,2} V. Martín-Mayor,^{3,2} and S. Pérez-Gaviro^{4,2}

¹*Dipartimento di Fisica, INFN and SMC, U. di Roma La Sapienza, P.le A. Moro 2, Roma I-00185, Italy.*

²*Instituto de Biocomputación y Física de Sistemas Complejos (BIFI), Corona de Aragón 42, Zaragoza 50009, Spain.*

³*Departamento de Física Teórica I, Facultad de Ciencias Físicas, Universidad Complutense, 28040 Madrid, Spain.*

⁴*Departamento de Física Teórica, Universidad de Zaragoza, Zaragoza 50009, Spain*

(Dated: March 22, 2022)

We numerically study aging for the Edwards-Anderson Model in 3 and 4 dimensions using different temperature-change protocols. In $D = 3$, time scales a thousand times larger than in previous work are reached with the SUE machine. Deviations from cumulative aging are observed in the non monotonic time behavior of the coherence length. Memory and rejuvenation effects are found in a temperature-cycle protocol, revealed by vanishing effective waiting times. Similar effects are reported for the $D = 3$ site-diluted ferromagnetic Ising model (without chaos). However, rejuvenation is reduced if off-equilibrium corrections to the fluctuation-dissipation theorem are considered. Memory and rejuvenation are quantitatively describable in terms of the growth regime of the spin-glass coherence length.

PACS numbers: 05.70.Ln, 75.10.Nr, 75.40.Mg

I. INTRODUCTION

Nowadays the arena for comparisons between theory and experiments in spin-glasses physics¹ is out-of equilibrium dynamics.² Spin-glasses *age*,³ as shown by the thermoremanent magnetization: consider a spin-glass that has spent a time t_w below its glass temperature, T_c , in the presence of a magnetic field. Let t be the time elapsed since the magnetic field was switched-off. The magnetization decays as a function of t/t_w^μ , even for $t_w \sim 1$ day. The exponent μ could be 1 (*full-aging*),⁴ although there are recent experimental claims for μ being smaller than 1 (*subaging*).⁵ A somehow complementary experiment consists in keeping the system for t_w below its glass temperature. Then, a magnetic field is switched on and the so-called zero-field cooled (ZFC) magnetization is recorded while it grows.⁴⁵ Full aging can be also observed in the a.c. magnetic susceptibility, $\chi(\omega, t_w)$ which, for a fixed ω , decreases as t_w grows. This time decay can be rescaled as a ω -independent function of ωt_w ,² although, experimentally, one is restricted to the range $\omega t_w > 1$.

Memory and *rejuvenation*^{6,7} are sophisticated manifestations of aging in experiments where the temperature is not kept constant. Rejuvenation arises when changing temperature from T_1 to T_2 (T_1 and T_2 smaller than the critical temperature, T_c) a system that has spent some time at T_1 , so that $\chi(\omega, t_w)$ barely depends on t_w . Just after the $T_1 \rightarrow T_2$ change, aging restarts. The imaginary part of the susceptibility suddenly grows then relax. The t_w dependency of $\chi''(\omega, t_w)$ gets stronger, as for a *younger* system. Rejuvenation means that the relaxation of $\chi''(\omega, t_w)$ is very similar to the one of a system just quenched from $T > T_c$ to T_2 . Sometimes it is said that the relaxation is identical to the one of a system instantaneously quenched to T_2 from infinite temperature (in Sect. IIIB, below, we elaborate on the different meaning of *instantaneous temperature quench* in a experiment and in a computer simulation). If the susceptibility

just after the quench to T_2 rises *above* the final value it had at T_1 , one speaks of *strong rejuvenation*.⁸ On the other hand, when the system is put back at temperature T_1 , $\chi''(\omega, t_w)$ continue its relaxation where it left it just before the temperature change (*memory effect*). These effects can also be observed in the real part of the susceptibility (see e.g. Fig. 1 of Ref. 9), although rejuvenation is very diminished as compared with the imaginary part. With the sophisticated *dip-experiment* temperature-change protocol,⁶ memory and rejuvenation are truly spectacular.

Memory and rejuvenation have been found in systems quite different from spin-glasses (see, however, Ref. 10). Examples are structural glasses¹¹, polymers (PMMA^{13,14}), and systems not particularly glassy (or not widely recognized as such), like colossal magnetoresistance oxides.¹⁵ Moreover, a disordered ferromagnetic alloy,¹² becoming spin-glass at lower temperatures, has shown rejuvenation and memory, through the dip-experiment protocol (although in this case memory could be easily erased by lowering the temperature). Spin-glasses display the quantitatively stronger effects, but it is unlikely that the physical mechanism underlying memory and rejuvenation are specific of spin-glasses.

The above definitions for memory and rejuvenation need qualification. Under very small temperature changes¹⁶ (say $\frac{T_1 - T_2}{T_1} < 5 \times 10^{-3}$) the behavior of the spin-glass is rather smooth. On the other hand, sharp memory and rejuvenation can be observed¹⁷ for $\frac{T_1 - T_2}{T_1} \sim 0.07$. The crossover from small to drastic effects is rationalized using *effective isothermal waiting times*.^{16,18} Consider the simplest temperature change protocol: a system is aged for time t_w at temperature T_1 , then its temperature is suddenly shifted from T_1 to T_2 . After the shift, the ZFC magnetization is measured. The effective time, $t_{T_2}^{\text{eff, shift}}$, is the age of the isothermally aged system at temperature T_2 , whose ZFC magnetization⁴⁶ is most similar to the one of the temperature-shifted system (the

two relaxations are not identical¹⁶). Rejuvenation arises when $t_{T_2}^{\text{eff,shift}}/t_w$ is below experimental resolution.

Similarly, one can define¹⁸ an effective time for the temperature cycle protocol $T_1 \rightarrow T_2 \rightarrow T_1$:⁴⁷ one keeps the system a time t_w at T_1 , then shifts the temperature to T_2 , waits a time $t_2 \sim 20t_w$, shifts back the temperature to T_1 , switches on a magnetic field and then records the ZFC magnetization. The effective time $t_{T_1}^{\text{eff,cycle}}$ is obtained by looking to the system aged at temperature T_1 for a time $t_w + t_{T_1}^{\text{eff,cycle}}$ whose ZFC magnetization is most similar to the one of the temperature-cycled system. One has memory, as we defined it above, when $t_{T_1}^{\text{eff,cycle}}/t_2$ gets below experimental resolution. A large variety of spin-glasses experiments find^{5,18} for $T_1 > T_2$

$$\frac{t_{T_1}^{\text{eff,cycle}}}{t_w} = \exp \left[-\frac{T_1 - T_2}{x_0 T_2} \right], \quad (1)$$

with⁴⁸

$$x_0 \sim 10^{-2}. \quad (2)$$

The theoretical investigation of these phenomena is less advanced than its experimental counterpart. Memory and rejuvenation can be recovered in the dynamics of abstract energy-landscape models.¹⁹ However, one wants to reproduce these phenomena in the Langevin dynamics for the standard spin-glass model, the Edwards-Anderson (EA) model.¹ This dynamics for the EA model can only be investigated by Monte Carlo simulation. Yet, difficulties have arisen in numerical investigation of memory and rejuvenation.^{8,21,22,23,24} Furthermore, the progress achieved regards temperature-shift and temperature-cycle experiments. The dip-experiment protocol remains still as too complicated to be analyzed theoretically.

Experiments where $(T_2 - T_1)/T_1$ is very small can be accounted for by the *cumulative aging* scenario,^{16,18} consisting in the three following hypothesis:

1. Aging is ruled by the growth of a coherence length,²⁵ signaling the building of a spin-glass order. For isothermal aging, this length is named $\xi_T(t)$, t being the total time spent in the glass phase. This isothermal growth-law has been studied in experiments¹⁸ and simulations,^{28,29} although the measured $\xi_T(t)$ grows by an small factor in both cases. Numerically, a power law

$$\xi_T(t) = A_T t^{z(T)}, \quad z(T) = z_c \frac{T}{T_c}, \quad (3)$$

fairly fits the data. However, more complicated rules have been used.^{5,16,17,18}

2. The coherence-length always grows with time. It behaves continuously upon temperature changes.
3. Effective times follow from the *isothermal* growth of the coherence length. Consider a temperature

shift after aging for time t_w at T_1 . One has

$$\xi_{T_1}(t_w) = \xi_{T_2}(t_{T_2}^{\text{eff,shift}}). \quad (4)$$

A time t after the shift, the coherence length is

$$\xi^{\text{shift}}(t) = \xi_{T_2}(t + t_{T_2}^{\text{eff,shift}}). \quad (5)$$

Similar reasoning is used in the analysis of more complicated temperature-change protocols.

Eq.(4) is used in an indirect way, both in the analysis of simulations^{8,24} and experiments.^{16,17,18} Relations such as (3), obtained in a different experiment, are used to convert the measured effective times into length-scales and viceversa. It is difficult to find in the literature *direct* data on the behavior of the coherence length upon temperature changes. A nice exception are the simulations of Ref. 21 where Eq.(5) was directly checked. Those simulation spanned 10^5 Monte Carlo steps (MCS). For comparison with experiments, recall that $1 \text{ MCS} \sim 1 \text{ picosecond}$.

Memory and rejuvenation appear as hardly compatible with the cumulative aging. Experiments show¹⁶ that $\xi_{T_1}(t_w) < \xi_{T_2}(t_{T_2}^{\text{eff,shift}})$ when the measured effective times are converted in length-scales, both for $T_2 > T_1$ and $T_1 < T_2$, in contradiction with Eq.(4).

Two theoretical scenarios are currently being considered to account for memory and rejuvenation. Rejuvenation was interpreted in terms of temperature chaos,³³ namely extreme sensitivity of *equilibrium* states in the glass phase to small temperature changes. An overlap-length, $l_0(T_1, T_2)$, is postulated to exist. Features at scale smaller than l_0 are unaffected by a temperature change $T_1 \rightarrow T_2$ while at larger scales the system is completely reorganized. Rejuvenation is then attributed to large length scales and strong rejuvenation requires small l_0 . The ghost-domain scenario (see Ref. 17 for a recent account) allows to reproduce memory in the chaos scenario. The other scenario²⁰ is closer in spirit to cumulative aging. Rejuvenation after a negative temperature shift would arise from the so-called fast modes involving length-scales smaller than $\xi_{T_1}(t_w)$, that were equilibrated at T_1 but fall out of equilibrium at T_2 . Memory would arise from time and length scales separation: back to temperature T_1 , fast modes re-equilibrate very fast so that aging continues from the previous T_1 state.

However, when it comes to actual calculations, it turns out that no convincing memory and rejuvenation has been found in computer simulations of 3D spin-glass models, either with a two-temperatures^{8,21,23,24} or with a dip-experiment protocol.²² When the behavior of the coherence length is followed for times up to 10^5 MCS,²¹ Eqs.(4) and (5) are fulfilled even for $\frac{T_1 - T_2}{T_2} \approx \pm 0.33$. Consistently with this finding, when the temperature cycle protocol is analyzed in the EA model,^{24,26} the x_0 in Eq.(1) turns out to be of order 1 rather than of order 10^{-2} . Should x_0 not decrease significantly for larger times, the whole low-temperature phase of the EA model could be accounted for by cumulative aging (i.e. the low-temperature phase would not be a spin-glass phase).

This contradiction with experiments is puzzling. It could be indicating that the EA model lacks some crucial ingredient²² (maybe long-ranged dipolar interactions?). Or maybe memory and rejuvenation involve time and length scales inaccessible to present-day simulations. Indeed, experiments are performed on a time-scale which is about 10^8 times longer than typical simulations. Yet, experimentally,¹⁸ there are around $\sim 10^5$ spins in a coherent cluster (hence $\xi_T(t_w) \sim 40$ lattice spacings), while simulations achieve (see below) $\xi_T(t_w) \sim 10$ lattice spacings. When length scales are confronted, the differences with experimental conditions do not seem so dramatic.

As for higher space dimensions, a simulation²³ of the temperature cycle protocol for the 4D EA model, yielded strong rejuvenation (as defined in Ref. 8). Yet, results in full agreement with cumulative aging, Eq.(4), were reported for $\frac{T_1-T_2}{T_2} \approx \pm 0.125$ (the simulation time was smaller than 10^4 MCS). In the Migdal-Kadanof lattice,²⁷ where rather larger times can be simulated, rejuvenation was found for $\frac{T_1-T_2}{T_1} \sim 0.1$, suggesting that x_0 in Eq.(1), does depends on the age of the system.

In this work, we report simulations of a 3D (made with the SUE machine³¹) and a 4D EA model with *binary* (rather than *gaussian*^{21,22,23,27}) couplings. Our 3D simulations are three orders of magnitude longer than previous ones. We use real replicas²⁸ to study the coherence-length, that is directly calculated (not inferred from effective times), through the temperature changes. In a temperature-cycle protocol, clear memory and rejuvenation effects are found for large values of $\frac{T_2-T_1}{T_1}$ both in 3D and in 4D (sections III A and III B). We also observe strong rejuvenation (in the sense of Ref. 8), but only if we neglect corrections to the Fluctuation-Dissipation theorem.³⁴ The coherence-length is shown to *decrease* upon some temperature changes, in contradiction with cumulative aging. Moreover, a value $t_{T_1}^{\text{eff,cycle}}$ compatible with zero can be obtained for $T_1 = 0.9T_c$ and $T_2 = 0.4T_c$, which is to be expected in view of Eqs.(1) and (2) (sections III B and III C). Furthermore, we will show that the two-times dependency of the time correlation function can be accounted for with surprising accuracy by the coherence-length at the two relevant times, both for isothermal aging and for temperature-shift protocols (section III D). We perform exactly the same calculations for the 3D *ferromagnetic* site-diluted Ising model³⁰ (where, in the absence of frustration, chaos is absent), obtaining very similar results. Although temperature chaos is probably present in models for spin-glasses,^{27,35} our results in the site-diluted *ferromagnetic* Ising model suggest that it plays no role in producing memory and rejuvenation. This was maybe to be expected, since memory and rejuvenation is being found experimentally in materials where chaos in temperature seems to be absent or where a thermodynamic glass transition has never been found.^{11,13,14} Unfortunately, we have made no progress³² in the analysis of the dip-experiment protocol.

II. MODELS AND SIMULATIONS

Specifically, we consider Ising variables, $\sigma_i = \pm 1$, occupying the nodes of a (hyper) cubic lattice in 3D and 4D with nearest-neighbor, quenched disordered interactions. We report results for the spin-glass with random ± 1 couplings and the 3D site diluted Ising ferromagnet³⁰ (spins are lacking with probability $1-p$). We evolve the system using a sequential, local heat-bath dynamics. Our time-unit (1 MCS ~ 1 picosecond) is a full-lattice update. For the spin glass we studied the lattice size $L = 60$ in 3D (mostly in SUE), and $L = 20$ for 4D (on PC clusters) with some tests in $L = 30$ finding no differences. For the site-diluted model we studied $L = 100$. The number of disorder realizations vary within 16 and 240.

In the following, we will call a *direct-quench* to the procedure of placing a fully disordered system (infinite temperature) instantaneously at the working temperature. This corresponds to an infinite quenching-rate.

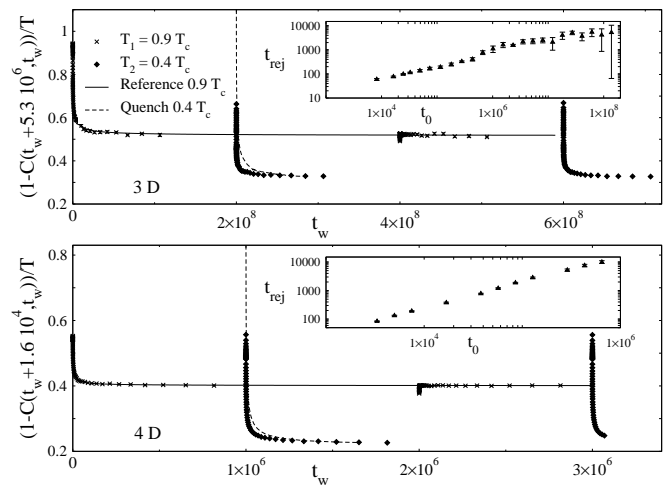


FIG. 1: **Top:** Naive $\chi(\omega = 2\pi/t_0, t_w)$, $t_0 = 5.3 \times 10^6$ for the 3D EA model vs. time. The T -cycle is $T_1 \rightarrow T_2 \rightarrow T_1 \rightarrow T_2$, each step lasting $t_s = 2 \times 10^8$. The full line is a reference run at $0.9T_c$. The inset shows the rejuvenation time (see text) vs. t_0 . The dashed line is a direct-quench to T_2 . **Bottom:** as top part for $D=4$, $t_0 = 1.6 \times 10^4$ and $t_s = 10^6$.

The Fluctuation-Dissipation Theorem (FDT) relates the autocorrelation function in zero magnetic field

$$C(t_w, t_w + t_0) = \frac{1}{V} \sum_i \langle \sigma_i(t_w) \sigma_i(t_w + t_0) \rangle \quad (6)$$

to the real part of the susceptibility: $\chi(\omega = 2\pi/t_0, t_w) \approx [1 - C(t_w, t_w + t_0)]/T$. Yet, off-equilibrium, FDT needs to be generalized replacing T by $T/X[C]$ ($X[C]$ is a smooth function³⁴ of $C(t_w, t_w + t_0)$). Hence, one assumes^{21,22,23,27} to be in pseudo-equilibrium regime ($\omega t_w \gg 1$ thus $X[C] = 1$), which is not always true. We also obtain *spatial* information from the correlation function of the overlap field, $q_i(t) = \sigma_i^{(1)}(t) \sigma_i^{(2)}(t)$, built from two independently evolving systems with the same

couplings, at the same temperature:

$$C_4(r, t_w) = \frac{1}{V} \sum_i \langle q_i(t_w) q_{i+r}(t_w) \rangle. \quad (7)$$

III. RESULTS

A. Strong rejuvenation?

In Fig. 1 is shown the time-evolution of the naive $\chi(\omega, t_w)$ (i.e. $[1 - C(t_w, t_w + t_0)]/T$) for the EA model in 3D (top) and 4D (bottom) for a (double) temperature cycle: $T_1 \rightarrow T_2 \rightarrow T_1 \rightarrow T_2$ ($T_1 = 0.9T_c$, $T_2 = 0.4T_c$). In 3D the system spends $t_s = 2 \times 10^8$ MCS at each temperature (1000 times longer than previous works), while in 4D $t_s = 10^6$ MCS. The results of a reference run, with temperature fixed to T_1 , are also shown (continuous line). When the temperature drops to T_2 , $\chi(\omega, t_w)$ increases over the reference curve and starts a new relaxation (*strong rejuvenation*⁸). When temperature is back to T_1 , $\chi(\omega, t_w)$ catches the reference run almost instantaneously (*memory*). We call t_{rej} to the time that the rejuvenated $\chi(\omega, t_w)$ is above the reference run (see insets in Fig. 1), that is found to grow consistently with t_0 (much faster in 4D). It is then conceivable that an effect of macroscopic time-duration could be observed (experiments explore $t_0 \sim 10^{13}$ MCS). However, specially in 3D, $t_{\text{rej}} < t_0$. This implies that this strong rejuvenation is confined to the regime $\omega t_w < 1$, which is out of reach for measurements of the a.c. susceptibility (note that strong rejuvenation is not always observed experimentally in the real part of the susceptibility⁹).

In agreement with Ref. 23, the relaxing curve after the temperature drop is independent of t_s on the explored range ($t_s = 10^6, 2 \times 10^7$ and 2×10^8 MCS in $D = 3$). Also shown in Fig. 1 is the relaxation of $\chi(\omega, t_w)$ for a direct-quench to T_2 (dashed-line). Such an infinitely-fast temperature drop is not realistic (see section III B). Anyhow, the relaxation is not identical to the one after the temperature shift, but the two become very similar (in $D = 3$, this happens for $t_w \sim 4t_0$). This is in marked contrast with previous simulations where $t_s \sim 10^4$ and $t_0 = 64$.⁸ For such a short times, one needs $t_w \sim 500t_0$ for the two relaxation curves to approach each other.

Yet, in Fig. 1 we assumed to be in pseudo-equilibrium regime. In order to estimate the FDT correction factor $X[C]$ we use the following procedure. We stay for time t_s at T_1 , then change temperature to T_2 , wait for time t_w and switch-on a small uniform magnetic field ($h = 0.03$). We then record the magnetization, $m(t_w + t)$, and $C(t_w, t_w + t)$. The sought $X[C]$ factor is obtained drawing $\chi T = m(t + t_w)T/h$ versus $C(t_w, t_w + t)$ (insets of Fig. 2). The resulting plot, t_w -independent for large t_w ,³⁴ can be fitted with two straight-lines, yielding $X[C]$. In Fig. 2 (top) we show the time evolution of the $\chi(\omega, t_w)$ for the same cycle as Fig. 1 with $t_s = 2 \times 10^7$. Correcting with $X[C]$ reduces rejuvenation to the point

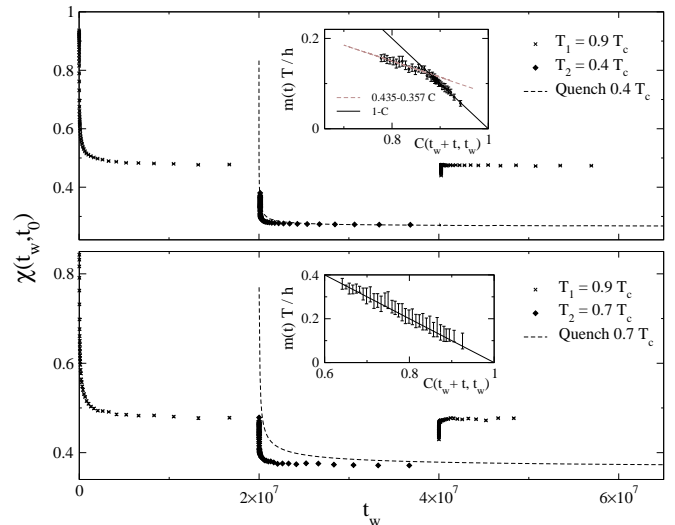


FIG. 2: **Top:** As Fig. 1 for $t_0 = 4.3 \times 10^5$ and $t_s = 2 \times 10^7$ but correcting FDT violations. *Inset:* Off-equilibrium fluctuation dissipation relation (see text). Data can be nicely fitted to two straight lines. **Bottom:** As in top part for $T_2 = 0.7T_c$. Only the pseudo-equilibrium regime is explored in this case (inset).

that *strong rejuvenation* is no longer seen. The susceptibility no more grows at the temperature drop to T_2 , although the relaxation restarts and still collapses appreciably with the $\chi(\omega, t_w)$ curve obtained from a direct-quench. Similar conclusions are drawn in 4D.³² We report in Fig. 2 (bottom) results for a cycle with a smaller temperature step ($T_1 = 0.9T_c$, $T_2 = 0.7T_c$). Here, (see inset), we stay in pseudo-equilibrium regime and rejuvenation is *stronger* for the smaller temperature drop, once the correcting $X[C]$ factor is considered. However the collapse with the direct-quench curve starts only for $t_w \sim 20t_0$.

1. The diluted ferromagnet

Memory and rejuvenation have been found in other systems than spin-glasses. A disordered ferromagnetic alloy,¹² becoming spin-glass at lower temperatures, has shown rejuvenation but much weaker memory, through the dip-experiment protocol. For comparison, we have simulated a site-diluted Ising model for $p = 0.395$ (T_c is accurately known³⁰). All the interactions being ferromagnetic, there is no temperature chaos in this system. We have simulated a $L = 100$ system checking that $\xi_T \ll L$ in our simulation window. We measure the naive susceptibility with the autocorrelation function (6). Just for fun, we try a three steps protocol, $T_1 = 0.9T_c \rightarrow T_2 = 0.7T_c \rightarrow T_3 = 0.4T_c \rightarrow T_2 \rightarrow T_3$, staying $t_s = 10^5$ MCS at each temperature. The results are shown in Fig. 3 (bottom) together with the results for an equal protocol for the 3D EA model (Fig. 3, top).

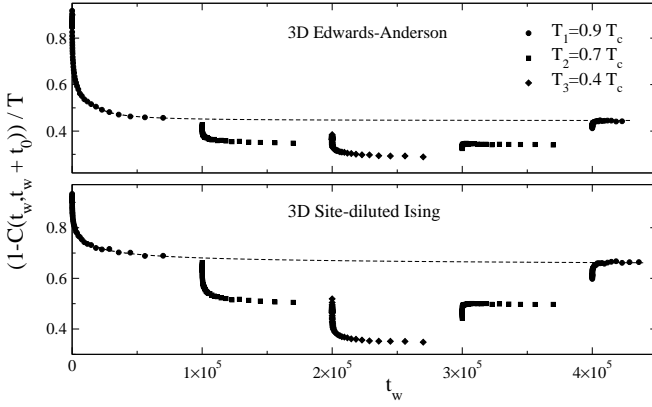


FIG. 3: Naive susceptibility in a 3 temperatures protocol (see text for details), for the binary EA $D = 3$ model (**top**) and the $D = 3$ site diluted ferromagnetic Ising model (**bottom**). The dashed line is a direct-quench to T_1 .

In both cases rejuvenation and a *double* memory are observed. Also in two temperature cycles³² the susceptibility behaves as in the EA model. To this level of analysis, there is no clear difference between the Edwards-Anderson model and the site-diluted Ising model.

B. Comparison with *experimental* direct-quench

In view of Eqs.(1) and (2), and the large temperature drop that we are studying, one would expect a perfect rejuvenation effect. However, Figs. 1 and 2 show that the relaxation after the first step at $0.9T_c$ considerably differs from the direct-quench (although this difference is smaller than for shorter simulations^{8,21}). This seems in plain contradiction with experiments (see e.g. Fig. 4 of Ref. 17). Yet, upon reflection, one realizes that the experimental direct-quench bears little resemblance with the simulational one. In fact, the experimental sample that is “instantaneously” quenched to $0.4 T_c$, expends at least 10 seconds ($\sim 10^{13}$ MCS!) in the spin-glass phase.

In order to make a fair comparison with experiments, one should study the relaxation after a “soft” quench (Fig. 4) from high-temperature to the working temperature below the glass transition. Yet, the fastest quenching rate that can be achieved in experiments is far too slow to be reproduced in present-day computers. To achieve a very slow temperature drop from high temperature to working temperature, it is useful to consider Fig. 1 in a different way. One realizes that the system that has spent $t_s = 2 \times 10^8$ MCS at $0.9T_c$, then suffers an instantaneous temperature drop to $0.4T_c$ is a better approximation to the experimental direct-quench to $0.4T_c$. In fact, the system spends quite a long time close to the critical temperature, where the time evolution —recall Eq.(3)— is faster. When looking to the double temperature cycle in Fig. 1, one needs to compare the relaxation in the first and in the second steps at $0.4T_c$, the first

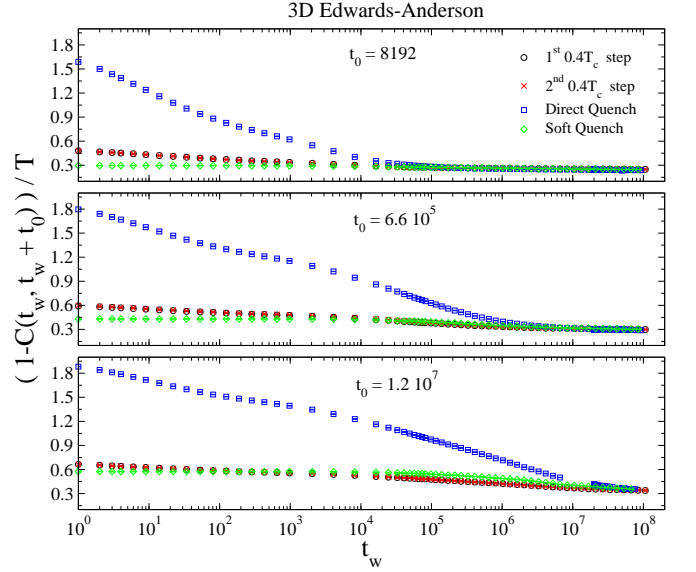


FIG. 4: (Color online) Naive $\chi(\omega = 2\pi/t_0, t_w)$ of the 3D EA model vs. time, at temperature $T_2 = 0.4T_c$, for several values of t_0 and thermal histories. In all cases, t_w is measured from the time of the (last) instantaneous quench to T_2 . **Squares** correspond to the instantaneous drop from infinite temperature to T_2 . **Circles** correspond to the system that has spent $t_s = 2 \times 10^8$ MCS at $T_1 = 0.9T_c$, then suffers an instantaneous quench to T_2 . **Crosses** correspond to the system that has been a time t_s at T_1 , then time t_s at T_2 , then time t_s at T_1 and finally suffers the instantaneous quench to T_2 . **Diamonds** correspond to a gradual drop from $9T_c$ to T_2 in 20000 MCS (we incremented $1/T$ in $0.113/T_c$ every 10^3 steps, the system spending 1.2×10^4 MCS in the spin-glass phase).

corresponding to the *reference* direct-quench, the second being looked at as the *temperature-cycled* system. This comparison is shown in Fig. 4, together with the relaxation after a *soft-quench*.

The frequencies shown in Fig. 4 span three orders of magnitude. In all cases, the relaxation for the softly-quenched system,⁴⁹ that has spent 1.2×10^4 MCS in the spin-glass phase, is much closer to the one of the cycled-system than the one of infinite quenching rate. Furthermore, the relaxations for the first and the second steps at $0.4T_c$ are identical, up to our statistical accuracy (see Fig. 5). This you may wish to call *perfect rejuvenation*.

In Fig. 5 we perform a detailed comparison between the soft-quench (with two quenching rates) and the two-steps protocol. To have a feeling of the frequency dependence, we show the smallest and the largest frequencies in Fig. 4. For very short times, in the two-steps protocols we find a quick decay of the susceptibility due to the sharp temperature drop. On the other hand, the softly-quenched system shows a basically constant behavior (the slower the quench, the lower the initial plateau is). When time becomes of the order of the total time spent in the spin-glass phase during the soft-quench, the susceptibility starts to decay and becomes very similar to the two-steps protocol. At $t_0 = 8192$, the two soft-

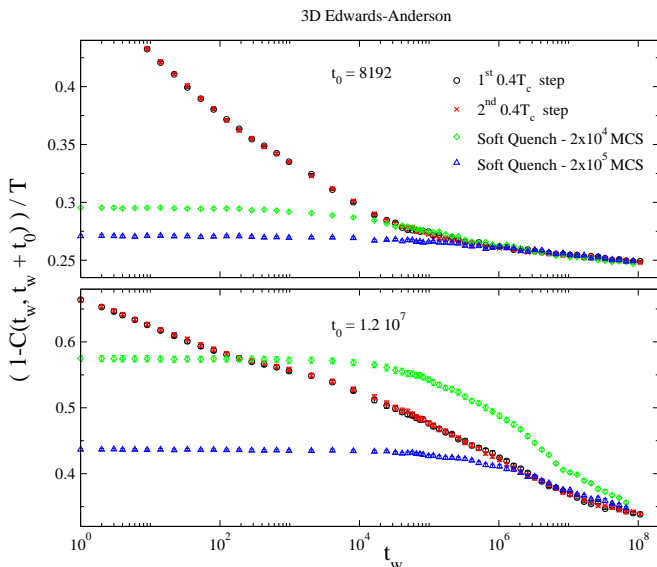


FIG. 5: (Color online) Close-up to the top and bottom panels of Fig. 4, excluding the data for the instantaneous drop from infinite temperature to $T_2 = 0.4T_c$. We also include data (**triangles**) for a still slower drop from $9T_c$ to T_2 in 200000 MCS (we incremented $1/T$ in $0.113/T_c$ every 10^4 steps, so that the system spends 1.2×10^5 MCS in the spin-glass phase).

quenches catch the relaxation of the two-step protocol and become identical. At the smallest frequency, the fastest quench approaches but does not catch the two-steps relaxation. On the other hand, for the smallest quenching rate, the relaxation curve becomes identical to the one of the two-steps protocol for $t_w \gtrsim t_0$, which corresponds to the experimentally accessible time range.

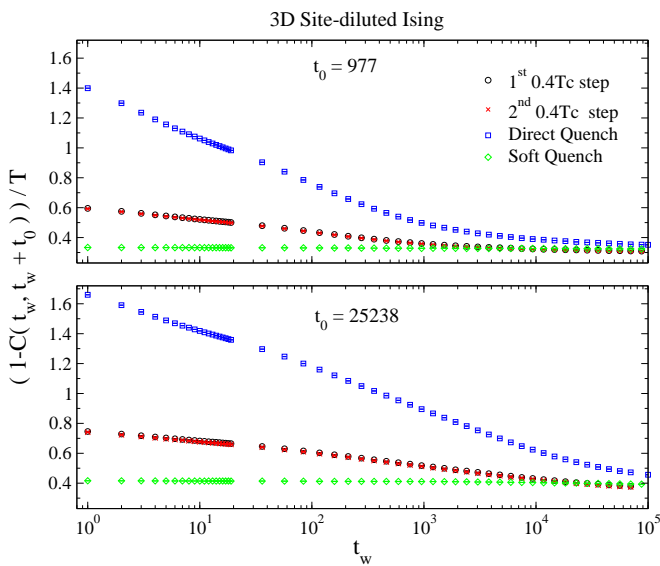


FIG. 6: (Color online) As in Fig. 4, for the diluted ferromagnet and $t_s = 10^5$ MCS. **Diamonds** correspond to a gradual drop from $9T_c$ to T_2 in 20000 MCS (we incremented $1/T$ in $0.117/T_c$ every 10^3 steps).

Quite similar results are obtained for the diluted ferromagnet, as we show in Fig. 6. Although it cannot be noticed at the scale of this plot, the relaxations in the first and second temperature-step are not identical for the Ising model. They may be made to collapse if the times in the second step are rescaled by a factor of 1.2 (in a protocol $0.7T_c \rightarrow 0.4T_c \rightarrow 0.7T_c \rightarrow 0.4T_c$, the needed rescaling factor is 2).

C. The coherence-length

The coherence-length may play a crucial role²⁰ in this physics, and should be followed in detail during temperature changes. This was done previously in Ref. 21, for times up to 10^5 MCS. Results in agreement with Eq.(5) were reported. We show here qualitatively different results for our longer simulations in 3D.

The coherence-length may be obtained from non self-averaging integrals of $C_4(r, t_w)$ using a second-momentum estimator.^{36,37} Not having so many samples at our disposal, we have obtained $C_4(r, t_w)$ (which is self-averaging for not very large r). The resulting curve has been fitted to²⁸

$$C_4(r, t_w) = \frac{A}{r^\alpha} \exp \left[- \left(\frac{r}{\xi(t_w)} \right)^\beta \right]. \quad (8)$$

In 3D, we find fair fits in the range $2 < r < 20$, fixing $\alpha = 0.65$ and $\beta = 1.7$ for all times and temperatures. The constant behavior of α does not agree with the results for the 4D model with Gaussian couplings.²³ To estimate errors in the three parameters fit (8) is very difficult. To have a feeling of their magnitude, let us report that $\alpha = 0.7$ yields good fits as well, with a 10% increased ξ estimate.

See in Fig. 7 (top), $\xi(t_w)$ for a direct-quench to $T_2 = 0.4T_c$ and for a thermal cycle $T_1 \rightarrow T_2 \rightarrow T_1$ with $T_1 = 0.9T_c$ and $t_s = 2 \times 10^7$. A power law with exponent ~ 0.144 fits nicely $\xi_{T_1}(t_w)$ for $t_w < t_s$, while the exponent for the direct-quench to T_2 is ~ 0.065 (full-lines in Fig. 7-top). Note that the exponent follow Eq.(3). During the T_2 -step, ξ grows over the T_1 value, and it is larger than for the direct-quench to T_2 . However, ξ decreases when the system is back to T_1 . Memory is striking: data for the second T_1 step, if translated back t_s MCS, are on top of the fit (obtained for $t_w < t_s$!). Let us stress two points regarding this result:

1. The coherence-length can *decrease* upon temperature changes, violating cumulative-aging, Eq.(5), and in contradiction with the time and length scales separation scenario.^{20,38} However, the effect is not symmetrical for negative and positive temperature shifts, as it was inferred experimentally from effective-time measurements.¹⁶
2. The effective time for the temperature cycle is compatible with zero (within our accuracy). This im-

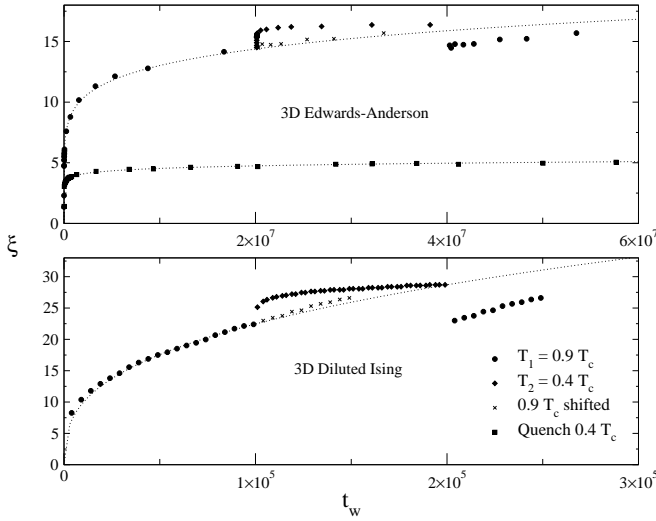


FIG. 7: **Coherence-length vs. time**, for the 3D EA model (**top**) and the diluted-ferromagnet (**bottom**). The thermal history has been a T -cycle $T_1 \rightarrow T_2 \rightarrow T_1$, being $t_s = 2 \times 10^7$ for the EA model and $t_s = 10^5$ for the Ising-diluted model. (*Crosses*: second T_1 -step data, translated back in time t_s ; *Dotted lines*: fits to $\xi(t_w) = At_w^x$ for $t_w < t_s$).

plies that, for $t_s \sim 10^7$, x_0 in Eq.(1) is *not* of order one, as it was found²⁴ for $t_s \sim 10^4$.

As before (bottom part of Fig. 7), the behavior of the diluted ferromagnet is completely analogous to the one of the EA model (including the power-law growth of $\xi_T(t)$).

D. The coherence length and two times correlations

A rather crucial feature of aging² is that two time-scales, t_0 and t_w , are involved. One would like to relate the *one* time quantity $\xi_T(t_w)$, to the *two* times correlation function. A crude estimate for $t_0 \gg t_w$ is

$$C(t_w, t_w + t_0) \propto \frac{\xi^{D/2}(t_w)}{\xi^{D/2}(t_w + t_0)}, \quad (9)$$

i.e. the coherent cluster that at time $t_w + t_0$ has linear size $\xi(t_w + t_0)$, at time t_w was composed of mutually incoherent clusters of linear size $\xi(t_w)$.

Indeed, (Fig. 8, top), the factor $\xi^{3/2}(t_w + t_0)/\xi^{3/2}(t_w)$ absorbs almost all the t_w and t_0 dependency of $C(t_w, t_w + t_0)$, both for a direct-quench to T_2 and for the T_2 part of the thermal cycle. Note that even the constant value for $C(t_w, t_w + t_0)\xi^{3/2}(t_w + t_0)/\xi^{3/2}(t_w)$ is equal for the direct-quench and for the thermal cycle. Also at T_1 , $C(t_w, t_w + t_0)\xi^{3/2}(t_w + t_0)/\xi^{3/2}(t_w)$ is constant within a band of width 5% of its mean-value.³² Quite similar results are obtained for the diluted ferromagnet, as we show in the bottom part of Fig. 8. In spite of the crudeness of the argument leading to Eq.(9) and the uncertainty in the determination of ξ , the results are surprisingly clear.

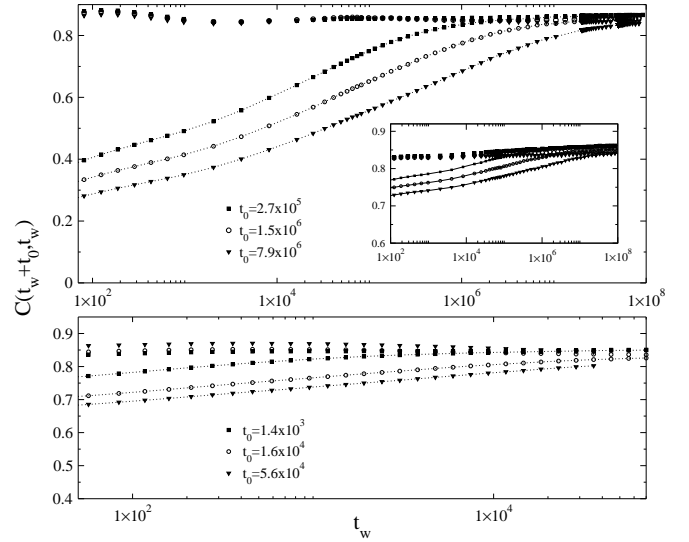


FIG. 8: **Top**: $C(t_w, t_w + t_0)(\xi(t_0 + t_w)/\xi(t_w))^{3/2}$ (points) and $C(t_w, t_w + t_0)$ (lines) vs. t_w , for the direct-quench to T_2 , for the EA model in 3D. *Inset*: As main plot for the T_2 step of the T-cycle of Fig.1. **Bottom**: As inset of top panel for the diluted Ising model.

Note that if Eq.(9) was *exact* the dynamics would be of the one-sector type,² which we do *not* believe to be the case.³⁹ Anyhow, given Eq.(9), full-aging⁴ is natural for a power-law growth of $\xi(t_w)$.

Thus, memory and rejuvenation are driven by the rate-growth of $\xi_T(t_w)$ rather than by its value or by the short-distance behavior of $C_4(r, t_w)$.^{20,23} In our simulation, rejuvenation is due to a *growth* of ξ upon cooling (probably, because of a sudden fall into a nearby energy minima), provoking a change in the evolution of $C(t_w, t_w + t_0)$. When temperature is shifted back to T_1 , ξ_{T1} continues its growth as if it had never being at T_2 with analogous consequences for the correlation-function (memory). This implies a non monotonic behavior of $\xi_T(t)$, in contradiction with cumulative-aging, Eqs.(4) and (5).

E. Results for $\omega t_w < 1$

Measurements of a.c. susceptibility are usually confined to the region $\omega t_w > 1$. On the other hand, thermal magnetoresistance measurements can yield information on the time regime $t_0 \gg t_w$. It is therefore worthwhile to have a look to our correlation functions in this regime.

The main issue here is the characterization of the time decay of correlations (see Ref. 39 for a recent study). One finds² that, at least when the correlation function lies in some intervals (say $C_1 < C(t_w, t_w + t_0) < C_2$), it behaves as a function of t_0/t_w^μ . It is possible that different intervals for the correlation functions (usually called *time-sectors*²) are ruled by different exponents. The existence of more than one time-sector is a necessary (but not sufficient) requirement for dynamic

ultrametricity.² Some indications of the presence of more than one time-sector in the dynamics of the EA model in 3D were found in Ref. 39.

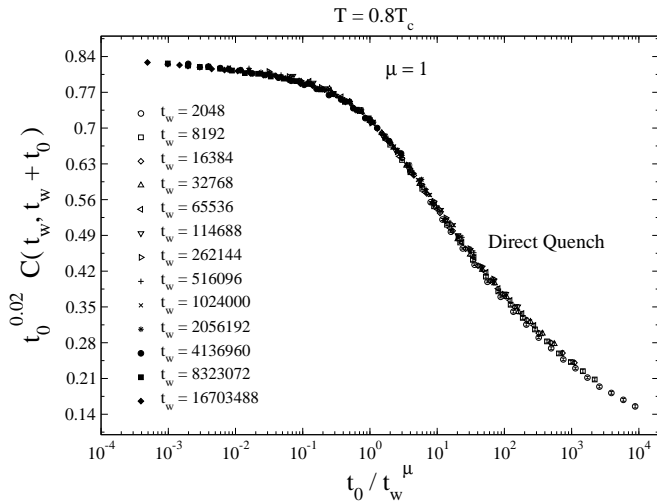


FIG. 9: Correlation function $C(t_w, t_w + t_0)$ scaled by $t_0^{0.02}$ (see Eq.(10)) after a direct-quench to $T = 0.8T_c$, versus t_0/t_w .

The experimental value of μ is controversial. Recently,⁴ it was claimed that it is $\mu = 1$ (full-aging). Previous failures in recognizing this, were ascribed to quenching-rate effects⁴ (recall also Sect. IIIB). In the quickest possible quench, $\mu = 1$ was clearly identified. This interpretation was recently disputed by the Saclay group,⁵ that find $\mu < 1$.

Regarding computer simulations, the following scaling form for the time correlation function was proposed,⁴⁰ and found to work for a restricted t_0 and t_w range:

$$C(t_w, t_w + t_0) = t_0^{-x(T)} \Phi\left(\frac{t_0}{t_w}\right). \quad (10)$$

This equation implies that full aging should be observed in the $t_0 \gg t_w$ regime. More recent and longer simulations³⁹ found deviations from Eq.(10), at least at some temperatures.

In Fig. 9 we plot our data for a direct-quench from infinite temperature to $0.8T_c$. Eq.(10) works nicely with $x(T) = 0.02$, which can be interpreted as evidence for full-aging behavior. However, at $T = 0.4T_c$ (see Fig. 10), we have been unable of finding a working $x(T)$. Actually, the relaxation is better interpreted in terms of two time-sectors: for $t_0 \gg t_w$, $\mu = 1$ seems to provide a proper scaling, while, at shorter t_0 , $\mu = 2/3$ does a better job.

In the inset of Fig. 10, we compare the relaxations at $T = 0.4T_c$ for the direct-quench and for the system that stayed 2×10^8 MCS at $0.9T_c$, then suffers a temperature shift to $0.4T_c$ (recall that this is our slowest quenching-rate from infinite temperature). For the slowly quenched system, the relaxation belongs to the $\mu = 2/3$ time-sector. Moreover, the relaxation after the

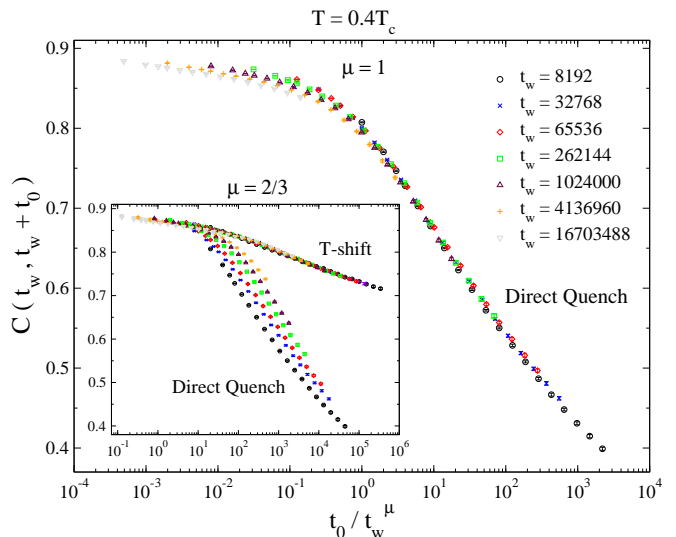


FIG. 10: (Color online) Correlation function $C(t_w, t_w + t_0)$ after a direct-quench to $T = 0.4T_c$, versus t_0/t_w . **Inset:** Data of main plot, versus t/t_w^μ , $\mu = 2/3$. We also plot data for a system that has been 2×10^8 MCS at $0.9T_c$, then suffers a temperature shift to $0.4T_c$.

T -shift provides a limiting curve, in the large t_w limit, for the $\mu = 2/3$ piece of the direct-quench relaxation.

At least within the time range that we can study, it seems that the quenching-rate does exert influence in the measured value of μ (as proposed in Ref. 4).

IV. CONCLUSIONS

In this work, we have compared memory and rejuvenation effects for the $D = 3$ and $D = 4$ binary EA model and for the $D = 3$ the site-diluted Ising model, finding quite similar results. Maybe the most important question we have addressed is whether the Edwards-Anderson model has a spin-glass low temperature phase, or not. The longer time scale reachable with the SUE machine³¹ (three orders of magnitude longer than previous work), has allowed us to conclude that spin-glass behave like experimental spin-glasses in a number of ways:

1. The relaxation of the a.c. susceptibility after a large temperature shift is as for a *direct-quench*, provide that one does not interpret the term *direct-quench* literally in the simulations (Sect.III B). We find little dependency in the previous thermal history, once microscopically short times are neglected.
2. Values of x_0 , defined in Eq.(1), are not of order 1 for waiting times $\sim 10^7$ MCS (contrary to the finding of Ref. 24 for waiting times of order $\sim 10^4$ MCS). This time dependence of x_0 is consistent with the findings in the Migdal-Kadanof lattice.²⁷

3. The coherence length may *decrease* upon temperature changes, in disagreement with the cumulative aging scenario, and in agreement with recent experiments.^{16,17}
4. The growth-rate of the coherence length rules the decay of the time-correlation function.²⁵ A very simple formula, Eq.(9), accounts for the behavior of $C(t_w, t_w + t_0)$ with surprising accuracy, for different temperature protocols. Contrary to the findings of short 4D simulations,²³ we do not find a strong temperature dependency of the replica-field correlation function, Eq.(7), at short distances. We rather ascribe rejuvenation to the coherence-length, which rules the long-distance behavior of the correlation-function.
5. The exponent μ for the t_0/t_w^μ scaling of the decay of $C(t_w, t_w + t_0)$, depends on the quenching-rate. In agreement with recent experiments,⁴ we find that the faster the quench is, the easier it becomes to obtain $\mu = 1$ (see, however, Ref. 5 for experiments contradicting this expectation).

The above findings suggest that the 3D EA model behaves as experimental spin-glasses do, contrary to what was inferred from previous shorter simulations.^{8,21,22,24} However, there are a few important differences. *First*, the out-of-phase and the in-phase susceptibility behaves quite differently in experimental spin-glasses (see e.g. Ref 9). This seems not to be the case for the EA model,^{8,24,32} within the accessible time-window. *Second*, the coherence-length is not found to decrease under positive temperature shifts, in contradiction with the inferred behavior from experimental measurements of effective-times.^{16,17} *Third*, in the dip-experiment protocol we have found³² no memory and very weak rejuvenation, in agreement with Ref. 22 even if we study frequencies 15 times smaller. *Fourth*, recent simulations do not^{24,41} find stronger memory and rejuvenation effects for Heisenberg than for Ising models of spin-glasses. This finding is in

contradiction both with experiments (see e.g. Ref.18) and with a recent calculation of overlap lengths in the Migdal-Kadannoff approximation.⁴² The physical reasons underlying these differences between our best model for spin-glasses and experimental spin-glasses are not yet understood. It is of course possible that longer times need to be studied. However, when time scales are converted to length-scales, one finds that numerical coherence-lengths are smaller than the experimental ones only by a small factor (see also Ref. 43).

We have shown that the ferromagnetic site-diluted Ising model (where chaos is absent) follows very closely the behavior of the EA model, at least in the $\omega t_w > 1$ regime. This is not totally unexpected, as we already know experimentally that systems quite different from spin-glasses show memory and rejuvenation.^{11,12,13,14,15} The natural conclusion is that chaos, although probably present in realistic spin-glasses,^{27,35,42} need not be invoked to explain memory and rejuvenation. However, it has been argued¹⁰ that the experimental protocol introduced in Ref. 16 may help to discriminate temperature chaos from a somehow trivial restarting of the dynamics (yet, see Ref. 44). More work will be needed to assess the usefulness of this new classification¹⁰ of aging systems.

V. ACKNOWLEDGMENTS

We thank G. Parisi, A. Tarancón, L.A. Fernández, F. Ricci-Tersenghi, E. Marinari, and A. Maiorano for discussions. Numerical simulations have been carried out in the dedicated computer SUE and in the PC clusters *RTN3* and *RTN4*, of U. de Zaragoza. S.J. and S.P.-G. acknowledge financial support from DGA (Spain) and (S.J.) from the ECHP programme, contract HPRN-CT-2002-00307, DYGLAGEMEM. This work has been financially supported by MEC (Spain) through research contracts FPA2000-0956, FPA2001-1813, BFM2003-08532 and FIS2004-05073-C04.

¹ See e.g. *Spin Glasses and Random Fields*, Ed. A. P. Young. World Scientific (Singapore, 1997).

² J.P. Bouchaud, L. Cugliandolo, J. Kurchan and M. Mézard, in Ref. 1; J.J. Ruiz-Lorenzo, *Advances in Condensed Matter and Statistical Mechanics*, Ed. E. Korutcheva, R. Cuerno, Nova Science Publishers (2004).

³ R.V. Chamberlin, M. Hardiman and R. Orbach, J. Appl. Phys. **52**, 1771 (1983); L. Lundgren, P. Svedlinsh, P. Nordblad, and O. Beckman, Phys. Rev. Lett. **51**, 911 (1983) and J. Appl. Phys. **57**, 3371 (1985).

⁴ At least for $10^{-2} < t/t_w < 10^2$, G.F. Rodriguez, G.G. Kenning, R. Orbach, Phys. Rev. Lett. **91**, 037203 (2003).

⁵ V. Dupuis, F. Bert, J.-P. Bouchaud, J. Hammann, F. Ladieu, D. Parker and E. Vincent, cond-mat/0406721.

⁶ K. Jonason, K. Jonason, E. Vincent, J. Hammann, J. P.

Bouchaud, and P. Nordblad, Phys. Rev. Lett. **81**, 3243 (1998).

⁷ L. Lundgren, P. Svedlinsh, O. Beckman, Journal of Magn. Magn. Mat. **31-34**, 1349 (1983); T. Jonsson, K. Jonason, P. Jönsson, and P. Nordblad, Phys. Rev. B **59**, 8770(1999); J.Hammann, E.Vincent, V. Dupuis, M. Alba, M. Ocio and J.-P. Bouchaud, J. Phys. Soc. Jpn. **69**, (2000) Suppl. A, 206-211.

⁸ H. Takayama and K. Hukushima, J. Phys. Soc. Jpn. **71**, 3003 (2002).

⁹ S. Miyashita, E. Vincent, Eur. Phys. J. B **22**, 203 (2001).

¹⁰ P.E. Jönsson, H. Yoshino, H. Mamiya and H. Takayama, Phys. Rev. B **71**, 104404 (2005).

¹¹ H. Yardimci, R.L. Leheny, Europhys. Lett. **62**, 203 (2003).

¹² E.Vincent, V. Dupuis, M. Alba, J. Hammann, J.-P.

- Bouchaud, Europhys. Lett **50**, 674 (2000).
- ¹³ L. Bellon, S. Ciliberto, C. Laroche, Eur. Phys. J. B **25**, 223 (2002).
 - ¹⁴ K. Fukao and A. Sakamoto, cond-mat/0410602.
 - ¹⁵ P. Levy, F. Parisi, L. Granja, E. Indelicato and G. Polla, Phys. Rev. Lett. **89**, 137001 (2002).
 - ¹⁶ P.E. Jönsson, H. Yoshino and P. Nordblad, Phys. Rev. Lett. **89**, 97201 (2002).
 - ¹⁷ P.E. Jönsson, R. Mathieu, P. Nordblad, H. Yoshino, H. Aruga Katori and A. Ito, Phys. Rev. B **70**, 174402 (2004).
 - ¹⁸ F. Bert, V. Dupuis, E. Vincent, J. Hammann and J.-P. Bouchaud, Phys. Rev. Lett. **92**, 167203 (2004).
 - ¹⁹ J.-P. Bouchaud and D.S. Dean, J. Phys. I (France) **5**, 265 (1995); M. Sales, J.-P. Bouchaud and F. Ritort, J. Phys. A: Math. Gen. **36**, 665 (2003); M. Sasaki, V. Dupuis, J.-P. Bouchaud and E. Vincent, Eur. Phys. J. B **29**, 469 (2002).
 - ²⁰ J.P. Bouchaud, *Soft and Fragile matter*, Eds: M.E. Cates, M.R. Evans (Institute of Physics Publishing, 2000).
 - ²¹ T. Komori, H. Yoshino, H. Takayama, J. Phys. Soc. Jpn. **69**, Suppl., 228 (2000).
 - ²² M. Picco, F. Ricci-Tersenghi, F. Ritort, Phys. Rev. B **63**, 174412 (2001).
 - ²³ L. Berthier, J.-P. Bouchaud, Phys. Rev. B **66**, 054404 (2002).
 - ²⁴ A. Maiorano, E. Marinari and F. Ricci-Tersenghi, cond-mat/0409577.
 - ²⁵ See L.W. Bernardi, H. Yoshino, K. Hukushima, H. Takayama, A. Tobo and A. Ito, Phys. Rev. Lett. **86**, 720 (2001), and references there in.
 - ²⁶ F. Ricci-Tersenghi, private communication.
 - ²⁷ M. Sasaki, O.C. Martin, Phys. Rev. Lett. **91**, 097201 (2003).
 - ²⁸ E. Marinari, G. Parisi, F. Ricci-Tersenghi and J.J. Ruiz-Lorenzo, J. Phys. A **33**, 2373 (2000).
 - ²⁹ T. Komori, H. Yoshino and H. Takayama, J. Phys. Soc. Jpn. **68**, 3387 (1999).
 - ³⁰ H. G. Ballesteros, L. A. Fernández, V. Martín-Mayor, A. Muñoz Sudupe, G. Parisi and J. J. Ruiz-Lorenzo, Phys. Rev. B, **58** 2740 (1998).
 - ³¹ A. Cruz, J. Pech, A. Tarancón, P. Téllez, C. L. Ullod and C. Ungil, Comput. Phys. Commun. **133**, 165 (2001).
 - ³² S. Jiménez, Ph.D. Thesis, U. Zaragoza, January 2005.
 - ³³ A.J. Bray, M.A. Moore, Phys. Rev. Lett. **58**, 57 (1987)
 - ³⁴ L. F. Cugliandolo, J. Kurchan Phys. Rev. Lett. **71**, 173 (1993); S. Franz, H. Rieger, J. Stat. Phys. **79** 749 (1995); E. Marinari, G. Parisi, F. Ricci-Tersenghi and J.J. Ruiz-Lorenzo, J. Phys. A: Math. Gen. **31**, 2611 (1998); D. Hérisson, M. Ocio, Phys. Rev. Lett. **88**, 257202 (2002).
 - ³⁵ T. Rizzo and A. Crisanti, Phys. Rev. Lett. **90**, 137201 (2003).
 - ³⁶ F. Cooper, B. Freedman, D. Preston, Nucl. Phys. **B210**, 210 (1989).
 - ³⁷ H.G. Ballesteros, A. Cruz, L. A. Fernández, V. Martín-Mayor, J. Pech, J. J. Ruiz-Lorenzo, A. Tarancón, P. Téllez, C. L. Ullod, and C. Ungil, Phys. Rev. B **62**, 14237 (2000).
 - ³⁸ Parametrizations of $C_4(r, t)$ different from Eq.(8) can be found, where ξ does not decrease (J.P. Bouchaud and L. Berthier, private communication).
 - ³⁹ S. Jiménez, V. Martín-Mayor, G. Parisi and A. Tarancón, J. Phys. A **36**, 10755 (2003).
 - ⁴⁰ H. Rieger, J. Phys. A **26**, L615 (1993); J. Kisker, L. Santen, M. Schreckenberg and H. Rieger, Phys. Rev. B **53**, 6418 (1996).
 - ⁴¹ L. Berthier and A.P. Young, preprint cond-mat/0503012.
 - ⁴² F. Krzakala, Europhys. Lett., **66**, 847 (2004).
 - ⁴³ Hukushima and Iba, preprint cond-mat/0207123.
 - ⁴⁴ L. Berthier and J.-P. Bouchaud, Phys. Rev. Lett. **90**, 059701 (2003).
 - ⁴⁵ The ZFC magnetization is a function of t/t_w^μ , t being measured from the instant when the magnetic field was switched on.
 - ⁴⁶ That is, one ages the system at T_2 for time $t_{T_2}^{\text{eff, shift}}$, then switches on the magnetic field and records the growing magnetization.
 - ⁴⁷ We somehow simplify the protocol description, for details see Ref. 18.
 - ⁴⁸ The actual value of x_0 depends both on T_1 and on the anisotropy of the microscopic spin-spin interaction (the more Heisenberg-like the interaction is, the smaller x_0 becomes¹⁸).
 - ⁴⁹ Soft-quench in this context actually means not infinite quenching rate, but dramatically faster than in experiments.